Edinburgh Research Explorer

Quantitative diagnostics of soft tissue through viscoelastic characterization using time-based instrumented palpation

CrossMark

Research Paper

Quantitative diagnostics of soft tissue through viscoelastic characterization using time-based instrumented palpation

Javier Palacio-Torralba[a], Steven Hammer[a], Daniel W. Good[b], S. Alan McNeill[b,c], Grant D. Stewart[b,c], Robert L. Reuben[a], Yuhang Chen[a,*]

[a]Institute of Mechanical, Process and Energy Engineering, School of Engineering and Physical Sciences, Heriot-Watt University, Edinburgh EH14 4AS, UK
[b]Edinburgh Urological Cancer Group, Division of Pathology Laboratories, Institute of Genetics and Molecular Medicine, University of Edinburgh, Western General Hospital, Crewe Road South, Edinburgh EH4 2XU, UK
[c]Department of Urology, NHS Lothian, Western General Hospital, Crewe Road South, Edinburgh EH4 2XU, UK

A B S T R A C T

Although palpation has been successfully employed for centuries to assess soft tissue quality, it is a subjective test, and is therefore qualitative and depends on the experience of the practitioner. To reproduce what the medical practitioner feels needs more than a simple quasi-static stiffness measurement. This paper assesses the capacity of dynamic mechanical palpation to measure the changes in viscoelastic properties that soft tissue can exhibit under certain pathological conditions. A diagnostic framework is proposed to measure elastic and viscous behaviors simultaneously using a reduced set of viscoelastic parameters, giving a reliable index for quantitative assessment of tissue quality. The approach is illustrated on prostate models reconstructed from prostate MRI scans. The examples show that the change in viscoelastic time constant between healthy and cancerous tissue is a key index for quantitative diagnostics using point probing. The method is not limited to any particular tissue or material and is therefore useful for tissue where defining a unique time constant is not trivial. The proposed framework of quantitative assessment could become a useful tool in clinical diagnostics for soft tissue.
© 2014 The Authors. Published by Elsevier Ltd. This is an open access article under the CC BY license (http://creativecommons.org/licenses/by/3.0/).

1. Introduction

Viscoelasticity in biological tissue was first recognized by Bayliss and Robertson (1939) in cat lungs. The time-dependent behavior in tissue has been attributed to the movement of fluid within its microstructure as in cartilage or liver (Huang et al., 2001; Kerdok et al., 2006) and also to the lubricating effect that the proteoglycan matrix exerts between the collagen fibrils that occur for example in blood vessels (Holzapfel, 2000). The mechanical behavior of collagen is also known to vary with strain rate (Bischoff, 2006), which is believed to contribute to the viscoelastic response of tissue such as lung (Ebihara et al., 2000), liver

(Garteiser et al., 2012), prostate (Phipps et al., 2005) and skin (Xu et al., 2007). Breast tissue has been observed to exhibit viscoelasticity which varies with conditions such as hormonal balance and disease (Balleyguier et al., 2013; Chen et al., 2013; Sack et al., 2013; Sinkus et al., 2005). The viscoelastic behavior of brain tissue (Guo et al., 2013; Rashid et al., 2014), has been shown to vary with pathological conditions such as multiple sclerosis (Streitberger et al., 2012), cancer and ageing (Sack et al., 2009). Liver tissue exhibits viscoelasticity (Kerdok et al., 2006; Taylor et al., 2002) that has been observed to vary, subject to diseases such as fibrosis (Salameh et al., 2007), water content (Kerdok et al., 2006) and preservation time (Yarpuzlu et al., 2014). Arteries have a rate-dependent behavior where the response is often anisotropic and nonlinear (Holzapfel and Gasser, 2000; Holzapfel et al., 2000). In cartilage, viscoelasticity is a desirable property allowing the stress associated with physiological work to be less damaging (Soltz and Ateshian, 1998). Muscular tissue also exhibits anisotropic viscoelasticity that becomes nonlinear at large strains (Takaza et al., 2013; Van Loocke et al., 2009). Thus, there is huge potential to use viscoelastic measurements in the assessment of the quality of soft tissue, in terms of a number of positive or negative physiological or pathological axes.

The elastic behavior of biological tissue has been thoroughly discussed in reviews (Ali et al., 2010; Beda, 2007; Boyce and Arruda, 2000) and can be described using such models as the 8-chain model (Bergstrom and Boyce, 2001) or other phenomenological continuum models such as Mooney-Rivlin (Palacio et al., 2013) or Ogden (Rashid et al., 2014). Viscoelasticity can be characterized using Prony series (Park and Schapery, 1999), Kelvin–Voigt fractional derivative (Taylor et al., 2002) and recruitment models (Bates, 2007). Of particular note is the work of Holzapfel and co-workers (Gasser and Holzapfel, 2002; Holzapfel, 2000; Holzapfel and Gasser, 2000; Holzapfel et al., 2000), who proposed viscoelastic models based on a strain energy density function of fiber-reinforced anisotropy that predicts the viscoelasticity of soft tissues such as arterial walls. Peña et al. (2010) also modeled the viscoelastic behavior of vascular tissue including the softening due to damage. Anisotropic viscoelastic models have also been proposed to predict the behavior of heart valves (Anssari-Benam et al., 2011). Bergström and Boyce (2001, 1997) described tissue viscoelasticity using the interaction between two networks, one related to the elasticity and the other to the viscous behavior. Although both networks have the same deformation gradient, the velocity gradient in the viscous network is decomposed into elastic and viscous velocity tensors. The so-called recruitment models consist of multiple Maxwell elements arranged so that, when a given element reaches the allowable strain, the following element starts to deform. Such models have proven successful in lung tissue, for example, where stress relaxation follows a power law (Bates, 2007).

The characterization of viscoelasticity for biological tissue requires the entire history of deformation in order to take into account its rate-dependency. Two different approaches are often adopted: creep/stress relaxation (quasi-static/low-rate) and dynamic tests. The results from quasi-static tests are often correlated by means such as Prony series (Brinson and Brinson, 2008), although other fitting techniques have been used, including a more generalized transfer function (between stress and strain) in Laplace space (Yu and Haddad, 1994), or using splines (Tran et al., 2011). These tests incidentally provide the instantaneous and the long-term moduli. In dynamic tests, the system (usually in a tension–compression configuration) is subjected to a pre-defined displacement function, such as a sinusoid. The amplitude of the force response and phase lag between the displacement and force signals can then be measured over a range of frequencies. In such tests, different techniques can be used to identify the corresponding transfer functions to relate the stress and strain in Laplace space (Renaud et al., 2011; Yu and Haddad, 1994).

It should be noted here that the two types of tests in fact measure the same thing, where the transfer function obtained from a stress relaxation/creep test mathematically dictates the dynamic behavior that would be measured in the frequency test, and *vice versa*. Therefore, the ranges of time and frequency that are used in any test may influence the results that are measured. For example, using higher frequencies or shorter times allows the detection of the smaller time constants that define the behavior during the early stage of stress relaxation, whereas lower frequencies provide information on the larger time constants that characterize the long-term response.

The time constants obtained from models such as Prony series define the characteristics of amplitude and phase-shift, but overfitting of a single data set using excess time constants can lead to undesired, sometimes entirely artificial, characteristics at certain frequency ranges. Therefore, it is critical to find the balance between the fitting error and the number of fitting parameters. Ideally the results of both dynamic and quasi-static tests should be fitted at the same time to avoid overfitting; however this would increase the complexity which becomes inapplicable for clinical tissue diagnostics.

Various types of medical devices have been reported for measurement of the mechanical properties of soft tissues. Oflaz and Baran (2014) designed a hand-held instrument to measure the *in situ* stiffness of biological tissues using a constant depth of indentation. A similar approach was proposed by Ahn et al. (2010), where the system remained attached to a movable cart. Indentation has also been used to measure the force–displacement behavior of tissues (Carson et al., 2011; Phipps et al., 2005). A less conventional approach was used by Ahn et al. (2012) where a device that mimics the sweeping palpation of the finger was developed. Sangpradit et al. (2011) presented a device for rolling tissue indentation again for application to tissue diagnostics. Some types of tissue have been adopted as candidates for diagnosis using direct or indirect mechanical palpation. Carson et al. (2011) and Ahn et al. (2010) used hemispherical indenters to measure the prostate stiffness *ex vivo*, which was then correlated to tissue quality. Mechanical approaches were also used to characterize swine brain *in vivo* (Miller et al., 2000), porcine (Ahn and Kim, 2010) and human (Carter et al., 2001) liver and skin, as well as soft tissue from lower limb extremities (Pailler-Mattei et al., 2008; Silver-Thorn, 1999).

Techniques for characterizing tissue *in vivo* have seen significant improvement during the last two decades, for example in prostate cancer diagnostics. Prior to the 1980s, most prostate biopsies were performed using a needle which was directly guided by the clinician (Sartor et al., 2008), largely relying on their experience of the anatomy. In the early 90s the technique was improved by the introduction of transrectal ultrasound (TRUS) guided biopsies and the sextant approach. The procedure is often repeated 10 to 12 times (up to 20) in different areas of the prostate, the samples then undergoing histological examination. However, despite these improvements, such an approach has some disadvantages such as false negatives (as the TRUS does not identify prostate cancer regions and the needle only samples small cores), pain and discomfort for the patient and the possibility of complications including rectal bleeding and hematuria Su (2010). The elastic behavior of the prostate is regarded as an important index in clinical diagnostics (Ahn et al., 2011; Carson et al., 2011; Hoyt et al., 2008; Masuzaki et al., 2007; Murayama et al., 2007), whereas its viscoelasticity has received less attention. Krouskop et al. (1998) reported a phase shift between stress and strain when prostatic tissue was dynamically examined at 0.1, 1 and 4 Hz. Carson et al. (2011) also showed that, when prostatic tissue is subjected to mechanical indentation, the required force depends on the velocity of indentation. Other studies by Phipps et al. (2005) and Hoyt et al. (2008) also indicated that the prostatic tissue (both healthy and diseased) exhibits phase shift and stress relaxation and therefore concluded that viscoelasticity could be of great importance in clinical assessment of tissue pathological conditions in the prostate.

Therefore, for prostate disease diagnosis, there is a clear need for an inexpensive, less invasive, fast and reliable method to improve quantitative assessment of tissue quality. In the more general framework of tissue diagnostics there is also an obvious need for quantitative methods through which the mechanical properties of the tissue can be related to its pathological condition. Some diagnostic techniques, such as elastography, already exploit the fact that relative change in mechanical properties is a good indicator of tissue quality, which could form the basis of an index for quantitative tissue diagnostics and enhance other diagnostic procedures, especially for *in vivo* recognition of cancerous nodules and pathological analysis.

This paper presents a framework for characterizing tissue viscoelastic properties as a diagnostic index of its pathological condition. The framework is applied to both healthy and cancerous prostates subject to dynamic mechanical palpation, with a view to forming general conclusions on the assessment of tissue condition and the identification of diagnostic parameters of cancerous nodules in soft tissue. As mentioned above, instead of requiring parameters from different viscoelastic material models, a set of generalized and simplified parameters is adopted for quantitative assessment of the tissue without *a priori* knowledge of its histology and pathology. The methodology and analysis of sensitivity to probe deployment options are explored by simulation in both 1D and 2D prostate models. The proposed method is then applied to a 3D model obtained from an MRI scan of an actual excised prostate.

2. Materials and methods

2.1. Viscoelastic models of biological tissue

The Zener model is one of the simplest rheological models for characterizing both creep and stress relaxation of viscoelastic materials and is adopted here to demonstrate the usefulness of time constants as indicators of rate-dependent behavior for quantitative tissue diagnostics. The model consists of a spring in parallel with a spring–dashpot series couple (Klatt et al., 2007; Renaud et al., 2011), and its stress–strain relationship can be expressed as

$$\frac{d\sigma}{E_2 \times dt} + \frac{\sigma}{\eta} = \left(1 + \frac{E_1}{E_2}\right) \times \frac{d\epsilon}{dt} + \frac{E_1}{\eta} \times \epsilon \qquad (1)$$

where E_1 denotes the stiffness of the single spring, and E_2 and η the stiffness and damping coefficient of the spring–dashpot couple, respectively. When the system is subjected to a uniaxial dynamic force $F = \sin(w \cdot t)$, the stress σ is $\sin(w \cdot t)/A$, where A is the area, w the angular frequency and t the time. Eq. (1) then becomes

$$c \times \cos(w \times t) + b \times \sin(w \times t) = s \times \frac{d\epsilon}{dt} + a \times \epsilon \qquad (2)$$

To simplify the notation: $a = E_1/\eta$; $b = 1/(\eta \cdot A)$; $c = w/A \cdot E_2$ and $s = 1 + E_1/E_2$. The solution of Eq. (2) is:

$$\epsilon(t) = K_1 \times e^{\frac{-E_1 \times t}{\eta \times s}} + P \times \sin(w \times t) + Q \times \cos(w \times t) \qquad (3)$$

where

$$P = \frac{c \times s \times w + b \times a}{a^2 + s^2 \times w^2} \qquad Q = \frac{a \times c - b \times s \times w}{a^2 + s^2 \times w^2}$$

and K_1 is to be obtained from boundary conditions. It is important to note that, if a dynamic displacement is used as the input, then the resulting differential equation is symmetrical, i.e. the typology of Eq. (2) is the same except the values of a, b, c and s therefore the solution for stress will be of the same form as Eq. (3).

Using Prony series, the transfer function of a viscoelastic material can be described as:

$$\sigma(t) = \int_0^t G(t - \tau) \times \frac{du(\tau)}{d\tau} \times d\tau \qquad (4)$$

$$G(t) = 1 - \sum_{i=1}^n D_i \times \left(1 - e^{-t/\tau_i}\right) \qquad (5)$$

which indicate that, to describe the behavior of a viscoelastic material, it is necessary to know the stress history which the material has experienced.

2.2. Quasi-static tissue characterization

The mechanical properties of prostatic tissue are known to change in the presence of benign prostatic hyperplasia (BPH) and cancer (Krouskop et al., 1998). For the sake of simplicity, mechanical properties of normal prostatic and cancerous tissue obtained from stress relaxation tests by Hoyt et al. (2008) are adopted in this paper. The relaxation curve is fitted by normalized Prony series in Fig. 1, using least squares approximation with a sufficient number of points based on the Kelvin Voigt Fractional Derivative (KVFD) model

(Hoyt et al., 2008). The least number of terms in Eq. (5) to fit the data adequately was found to be two; using a single term only allows fitting to either short or long time but not both. Table 1 shows the corresponding viscoelastic parameters, where D_i and τ_i are the constants to be determined in Eq. (5).

2.3. Dynamic tissue characterization

Dynamic characterization of viscoelastic tissue is usually performed by constructing phase and amplitude diagrams with respect to a range of frequencies and obtaining the parameters using a certain model (Martinez-Agirre and Elejabarrieta, 2011; Renaud et al., 2011). Alternatively, the storage and loss moduli that relate to the elastic and viscoelastic components can also be obtained in the same way (Madsen et al., 2005; Nayar et al., 2012).

In its simplest form, mechanical palpation involves imposing an input displacement from an indenter and measuring the corresponding reaction force. Without loss of generality, a sinusoidal displacement with a compressive mean position is chosen so that separation between tissue and indenter can be minimized. A smoothed mean value of the force signal $f(t)$ is obtained using a weighted local regression algorithm (LOESS) (Cleveland, 1979). By fitting f with a series of exponential functions as described below, a set of parameters: a_i, t_i, b_i can be obtained.
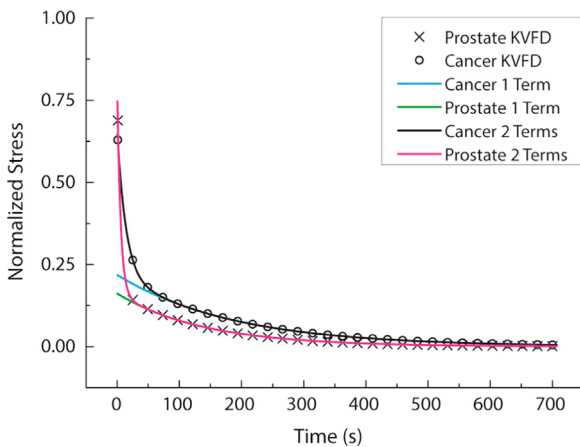

Fig. 1 – Prony series approximation of the normalized stress relaxation obtained from the model (Hoyt et al., 2008), using one or two terms. It can be observed that results using two terms present better fitting for both short and long term behaviors simultaneously.

$$f(t) = \sum_{n=0}^{i-1} \left(a_n \times e^{-t/t_n} + b_n \right) + a_i \times e^{-t/t_i} + b_i$$
$$+ \sum_{n=i+1}^{N} \left(a_n \times e^{-t/t_n} + b_n \right) \tag{6}$$

The parameters 'a' and 'b' are related to the material elasticity, b, in particular, being an index for the long-term elastic modulus. It should be mentioned here that the duration of the palpation experiment is critical in determining the reduced set of parameters. From Eq. (6) it can be seen that, for a given time of palpation, one time constant (t_i) will predominantly influence the viscous behavior of the material. Time parameters significantly higher than t_i (i.e. $n \geq i+1$) can be considered constants since their behaviors during short testing times are indistinguishable from an instantaneous modulus. On the other hand, smaller time parameters (i.e. $n \leq i-1$) will make the exponential term tend to unity which means that those terms will be added to the long-term modulus b_i. In both cases, b becomes an important index for apparent elasticity of the tissue.

2.4. Implementation of viscoelastic models

2.4.1. 1D mathematical model
The 1D model was created first to conduct a theoretical analysis that allows a better understanding of tissue viscoelastic behavior in both transient and steady state. A sinusoidal displacement was applied at one end of the model, which is fully fixed at the other. The cross-sectional area is A, Young's modulus E and the length L. For the sake of simplicity, it is assumed in this section that the viscoelasticity of prostatic tissue can be modeled by a Prony series with one time constant, which, after normalization, is given by:

$$E(t) = 1 - E_1 \times \exp\left(-\frac{t}{\tau_1} \right) \tag{7}$$

When subjected to a certain displacement, the reaction force is described as

$$F(t) = \frac{A}{L} \times \int_0^t \left(1 - E_1 \times e^{-(t-\xi/\tau_1)} \right) \times \frac{d(\sin(w \times \xi))}{d\xi} \times d\xi$$
$$= \frac{A}{L} \left(\sin(wt) - \frac{E_1 \tau_1 w \left(\cos(wt) - e^{-t/\tau_1} + \tau_1 w \sin(wt) \right)}{1 + \tau_1^2 w^2} \right) \tag{8}$$

Once the steady state is achieved the mechanical behavior is then governed by two oscillatory terms: a sine and a cosine, the latter of which accounts for the phase shift between input and output signals. The amplitude of the oscillations in steady state can be calculated as:

$$Amplitude = \sqrt{\psi^2 + \xi^2} \tag{9}$$

Table 1 – Material parameters for cancerous and healthy tissues fitted using Prony series. D_1/τ_1 are related to the short-time behavior and D_2/τ_2 to the long-term.

	KVFD model[26]	Prony series (fitted)				
	η (kPa s$^\alpha$)	α	D_1	D_2	τ_1 (s)	τ_2 (s)
Healthy	8.7±3.4	0.22±0.04	0.4432	0.2182	13.87	187.6
Cancer	3.6±1.3	0.23±0.03	0.63337	0.16144	5.4981	140.63

where ψ and ξ are the coefficients of the sine and cosine terms in Eq. (8) respectively, normalized with respect to E, A and L. The phase shift is calculated as

$$\Delta\phi = \mathrm{atan}\,\frac{\xi}{\psi} \qquad (10)$$

2.4.2. Prostate cancer diagnostics: 2D and 3D models

Finite element models were created to demonstrate the effectiveness of the proposed method in quantitative tissue diagnostics. A 2D model, representing a cross-section of *ex vivo* prostate sample, which is constrained at the bottom surface (opposite the indenter), was created first. An indenter with a hemispherical tip was modeled as a rigid solid, to which a sinusoidal displacement was applied. The prostate was then modeled in ABAQUS (Dassault Systemes, Vlizy-Villacoublay, France) and the material behavior was adjusted with a second order Ogden strain energy density function to mimic a linear viscoelastic material with an elastic modulus of 17 kPa for healthy tissue and 34 kPa for cancerous tissue, according to Table 1. The mesh under the indenter was refined to allow a better solution to the contact problem and inertial effects were taken into account using a tissue density of 1 kg/m^3 (Torlakovic et al., 2005).

A 3D prostate model was also created to provide a more realistic evaluation of the proposed methodology. The model was based on a prostate specimen, excised using the laparoscopic radical prostatectomy approach, from a patient undergoing surgery for localized prostate cancer. After removal of the prostate, a 7-T magnetic resonance imaging (MRI) was performed on the fresh specimen, using a resolution of 0.31 mm in the sagittal and coronal planes and 1.5 mm in the axial plane. In total, 44 images were obtained to reconstruct the 3D model using Scan-IP (Simpleware Ltd., Exeter, UK).

Fig. 2 summarizes the proposed methods for carrying out such a procedure in practice, where Fig. 2(a) shows the workflow to assess tissue quality from the MR imaging via viscoelastic characterization and Fig. 2(b) illustrates the set-up of *in situ* palpation of the reconstructed prostate model in comparison with the *ex vivo* measurement.

3. Results and discussion

3.1. Tissue characterization: 1D theoretical analysis

Clinical tissue diagnostics is a major challenge due to various complex constraints such as time, available number of samples, patient discomfort and pathological conditions. Therefore, it is critical to select the optimal measures (such as phase-shift and/or amplitude), and to choose the optimal parameters, such as frequency and number of measurement points. The 1D dynamic analysis was carried out using different time parameters across the available frequency scope in order to identify the optimal range of frequency over which a dynamic measurement should be performed. The range of frequency starts at 1 Hz, since lower values would lead to excessively long tests. The upper limit is determined by those which produce undesirable dynamic behavior and, in the extreme, data loss due to indenter lift-off if the sample is unable to recover its original shape when the indenter retracts.

Fig. 3 shows the amplitude and phase response from a sinusoidal displacement over a range of frequency using various viscoelastic parameters. It can be seen in Fig. 3(a) that viscosity plays very little role at low frequencies because the low velocity of deformation leads to the strain being effectively time-independent. Under such conditions the behavior can be characterized using the long-term modulus. Increasing the strain rate (frequency) amplifies the force amplitude and also the apparent stiffness until a plateau is reached. Materials with time constants
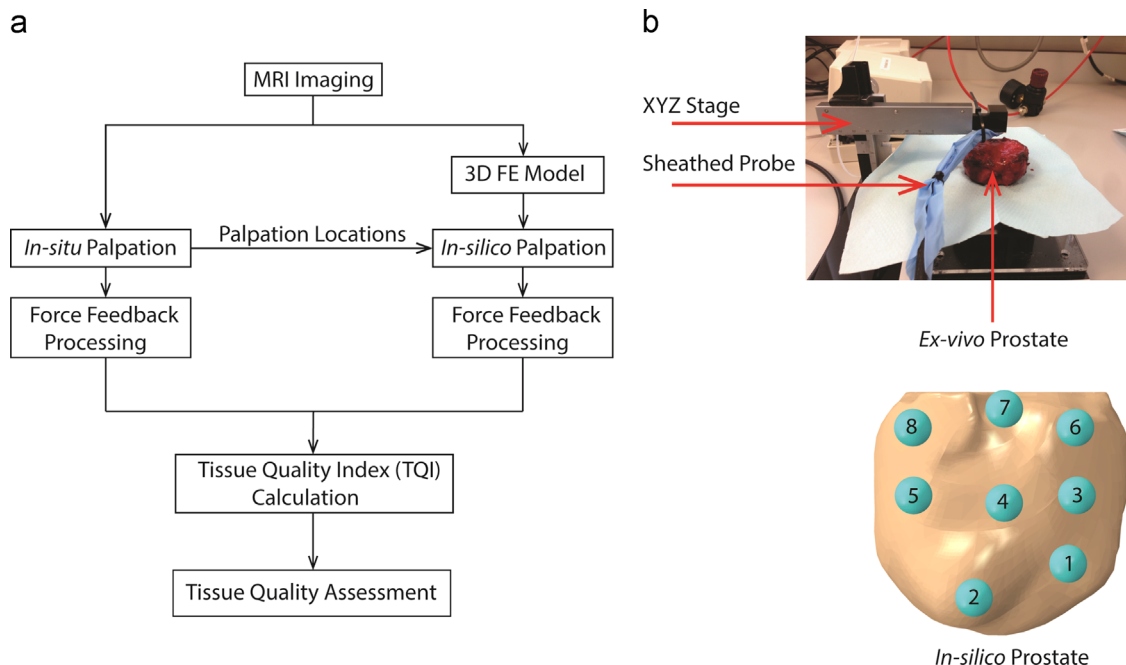

Fig. 2 – Schematic of the proposed methodology. (a) Flow chart of the proposed methodology. (b) Set-up of *in situ* palpation of the reconstructed prostate model in comparison with the *ex vivo* measurement.

τ in the range of 1 to 10 s exhibit primarily the instantaneous modulus when subjected to frequencies in excess of 1 Hz. The range of frequency where viscoelastic behavior of such materials exhibits is found to be between 0.001 and 1 Hz, as shown in Fig. 3. Therefore, the differentiation of the tissues which exhibit time constants consistent with the measurements of Hoyt et al. (2008) ($\tau_{Healthy} = 5.49$ s and $\tau_{Cancer} = 13.87$ s) would need to be based on their (quasi-)elastic behavior since frequencies lower than 1 Hz are not clinically practical. Such quasi-elastic behavior can also be observed in the phase lag diagram shown in Fig. 3(b), which tends to zero in the range of higher frequency (>1 Hz). To differentiate materials using phase lag their time constants should be at least one order of magnitude different. More importantly, to observe a noticeable phase shift, the material needs to have at least one time constant in the range of 0.001 s to 1 s.

Fig. 4 shows the amplitude and phase lag behavior of the prostatic and cancerous tissue when the dynamic behavior is fitted using a Zener model. The parameters of the Zener model are estimated by least squares fitting, using the quasi steady-state solutions to the reaction force from input (displacement) frequency at 0.1, 1, 10 and 100 Hz for both Prony and Zener models. Fitting the results, which are shown in Table 2, over a wide range of frequencies allows characterization of the dynamic behavior with a reduced risk of overfitting.

The viscoelastic behavior predicted by the Zener model is similar to that obtained using a Prony series, where a quasi-elastic response is evident at the extremes of high and low frequency illustrated by constant amplitude and negligible phase lag. The transition between the two states can be considered as the frequency range where dynamic measurements of viscoelastic properties can be made. The parameter that dictates this behavior is the time constant $\tau = \eta/E_2$, so it can be seen that the dynamically sensitive range runs between 0.001 Hz and 0.1 Hz for the case of amplitude and 0.001 and 1 Hz for the phase lag.

In this particular case, phase shift only becomes significant at frequencies below about 1 Hz when parameters from Hoyt et al. are adopted. In that case, unfortunately, the reaction force obtained will only depend on the long-term modulus and therefore only elasticity will be measured, losing most of the viscous information that the material presents.

3.2. Sensitivity analysis: 2D dynamic study

In a practical application of tissue diagnostics using mechanical probing, it would be rather difficult to perform palpation across the entire surface. Therefore a grid of test points would normally be used to assess the accessible surface. It
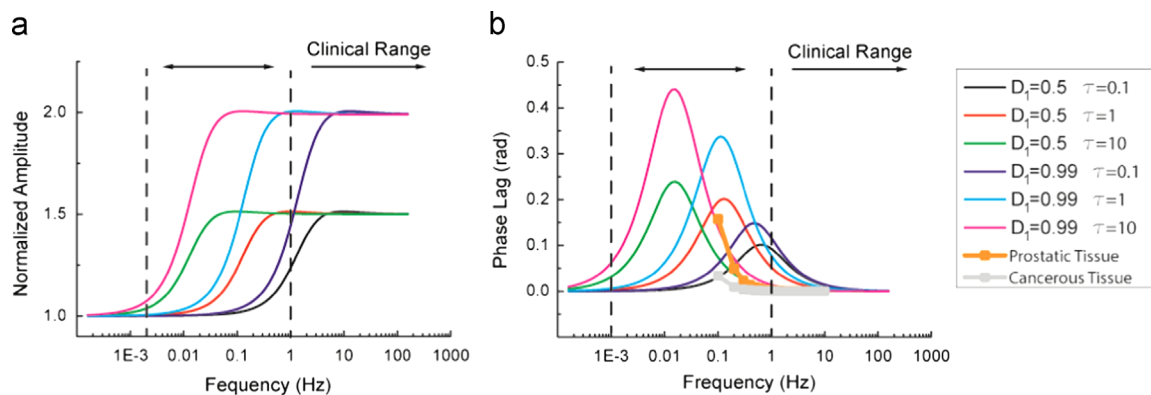

Fig. 3 – Mechanical behavior of tissues with different viscoelastic parameters subjected to dynamic palpation. (a) Evolution of relative amplitude with respect to frequency; and (b) phase shift between displacement and force signals, where phase lag of prostatic and cancerous tissues are also shown.
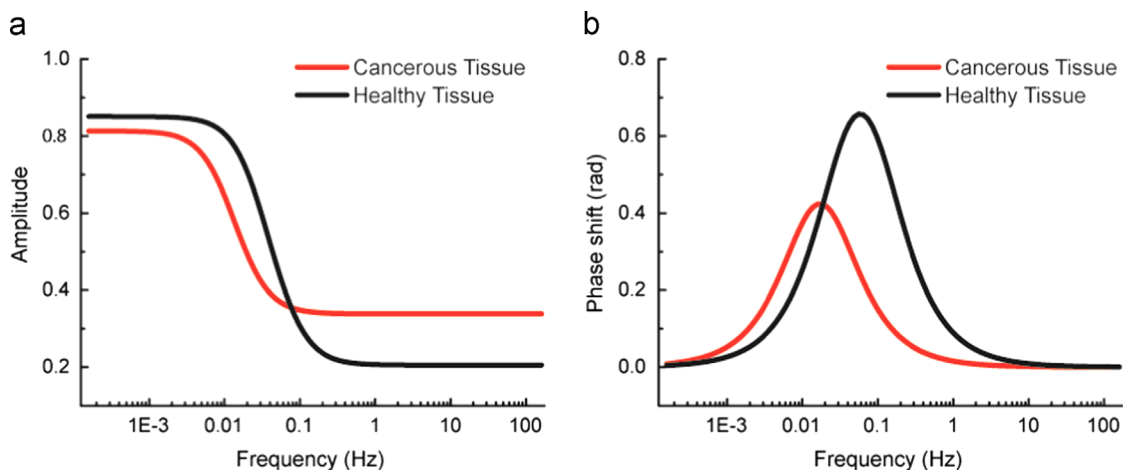

Fig. 4 – Amplitude and phase shift from Zener model using fitted parameters.

is useful to explore the sensitivity of the proposed method with respect to various diagnostic indices, such as position, depth and size of a cancerous nodule.

In this section the proposed method is applied to a 2D model with a representative cross-section of prostate sample where size, depth and position of a cancerous nodule vary. The displacement is applied to the prostate through an indenter, shown in Fig. 5 where stress distribution at different stages of indentation are illustrated, including initial contact in Fig. 5(b), mean position of indentation in Fig. 5(c) and lowest indentation point in Fig. 5(d). The stress becomes higher underneath the indenter and around the cancerous nodule when the indentation progresses, which leads to higher stress in a larger area and hence a larger reaction force, although there will be a limit to how deep an indentation can be made before discomfort or damage occurs. Increasing the mean depth of indentation for a given nodule size and position also increases the measured apparent stiffness, b, due to the increased strain and also the larger contact area of the indenter. Finally, excessively deep indentations cause an artificial increase in the measured stiffness due to the mechanical support at the bottom.

Fig. 6 illustrates the changes in viscoelastic parameters a, b and τ of a prostate when two different sizes of nodule (large, 6 mm in radius, and medium, 4 mm in radius) both located 12.5 mm under the surface are shifted horizontally in 5 mm increments away from the indenter. As shown, there is little discrimination when the nodule is far away from the indenter, which is to be expected since the disruption to the stress distribution caused by a distant nodule is small. Therefore, in order to assess tissue quality, a sufficient number of indentations needs to be used for lateral resolution/discrimination.

The effects of size and depth of the cancerous nodule are explored in Fig. 7, and found to have a substantial effect on both parameters a and b. The depth and size of a cancerous nodule are, in fact, coupled in the elastic response, which means that a smaller nodule close to the surface will lead to similar force feedback to a larger/deeper nodule. Therefore, in this case, the elasticity alone is unable to discriminate between size and depth, although changes in τ (hereinafter referred to as Tissue Quality Index, TQI) remains less affected in both cases, which implies that using relative changes of both tissue elastic and viscous behaviors may lead to decoupling of depth and size of cancerous nodule, thus making quantitative diagnostics possible.

3.3. Quantitative cancer diagnostics in prostate: A 3D study

In this section the proposed method will be applied to the 3D prostate model shown in Fig. 8(a), which is reconstructed from an excised prostate with the cancerous nodule closer to

Table 2 – Viscoelastic parameters of the equivalent Zener model.

Zener model parameters ($R^2 > 0.99$)

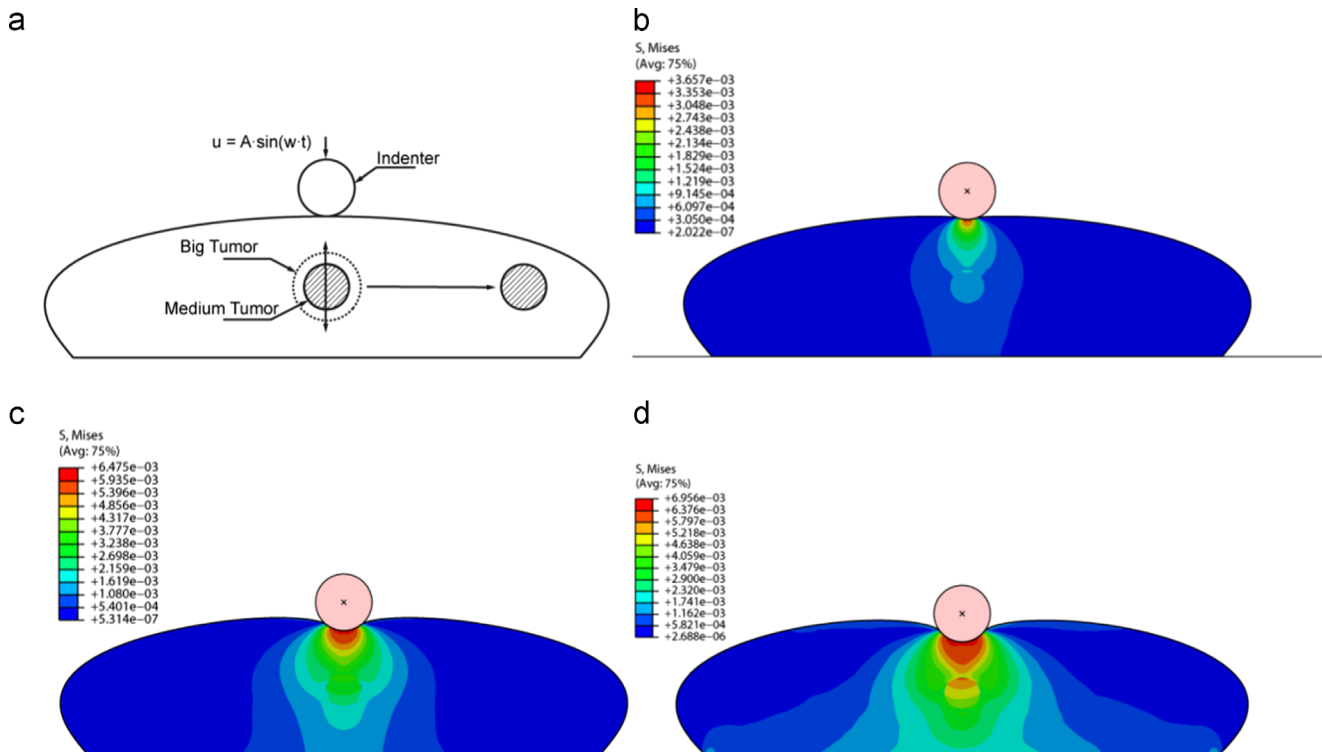|	E_1 (N/m)	E_2 (N/m)	τ (s)	η (N/m s)
Healthy	1.175	3.6985	4.9538	18.3216
Cancer	1.2294	1.7239	10.2925	17.7432

Fig. 5 – Sensitivity analysis of the proposed method. (a) Schematic diagram; (b) stress distribution when indentation occurs with a small nodule located at the center of the prostate; (c) at mean depth; and (c) at maximum depth. Unit of plotted stress is MPa.

the posterier side. The palpation area used in the model was on the posterior side of the prostate and was sequentially indented at 8 sites as shown schematically in Fig. 8(b). The indentation sites were selected to maximize the area to be tested across the entire surface whilst maintaining good contact between indenter and prostate. The anterior surface was constrained to mimic the *ex vivo* boundary conditions during an actual mechanical indentation. Fig. 8(c) and (d) show the recorded force in both healthy and cancerous samples and the fitted smoothed data used to determine the reduced set of parameters for tissue quality assessment.
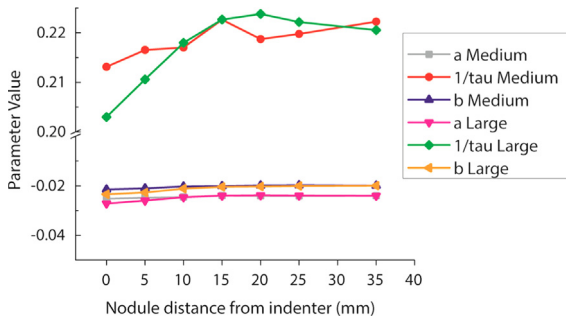

Fig. 6 – Sensitivity analysis for laterally positioned nodules.

It is evident that the displacement and force signals are hardly distinguishable and the difference becomes negligible especially during steady-state. This again indicates that only using phase shift and/or amplitude may not be sufficient to assess the tissue quality in a quantitative way.

In order to examine the applicability of the proposed method in 3D, two models are created here: one with a cancerous nodule inside which has the same viscoelastic parameters used earlier; another one which is fully healthy (material properties of healthy tissue are assigned to the cancerous nodule). The resulting viscoelastic parameters (i.e. a, b and τ) of the entire prostate are shown for both cases in Table 3. It is important to note here that, even in the healthy case, the reduced set of parameters does not remain constant at all probe points due to the surface curvature which changes the contact area and hence tissue response in the tissue-indenter contact zone, and therefore the force feedback. Nevertheless, at probe points 5, 6 and, 8, close to the nodule, the viscoelastic properties cause a stiffer and slower response for the prostate with the cancerous nodule. It is important to note that, as shown in Fig. 9, the tissue quality index offers a unique capability of quantitatively characterizing the location and extent of cancerous nodules inside the tissue.
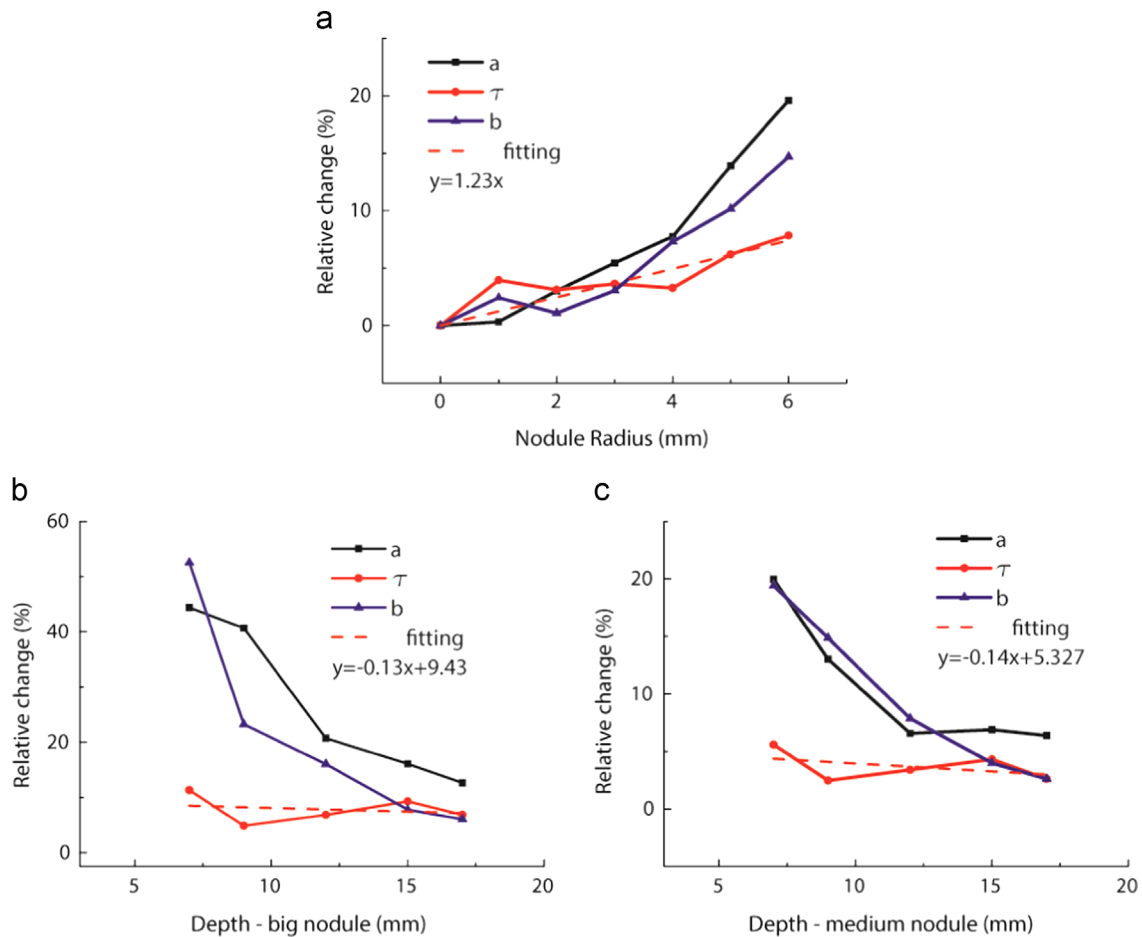

Fig. 7 – Sensitivity analysis: changing the depth, size and position of the cancerous nodule. (a) Evolution of model parameters when size of cancerous nodules varies. (b) and (c) show evolution of model parameters when depth of cancerous nodules varies in models with medium and big size nodule, respectively.
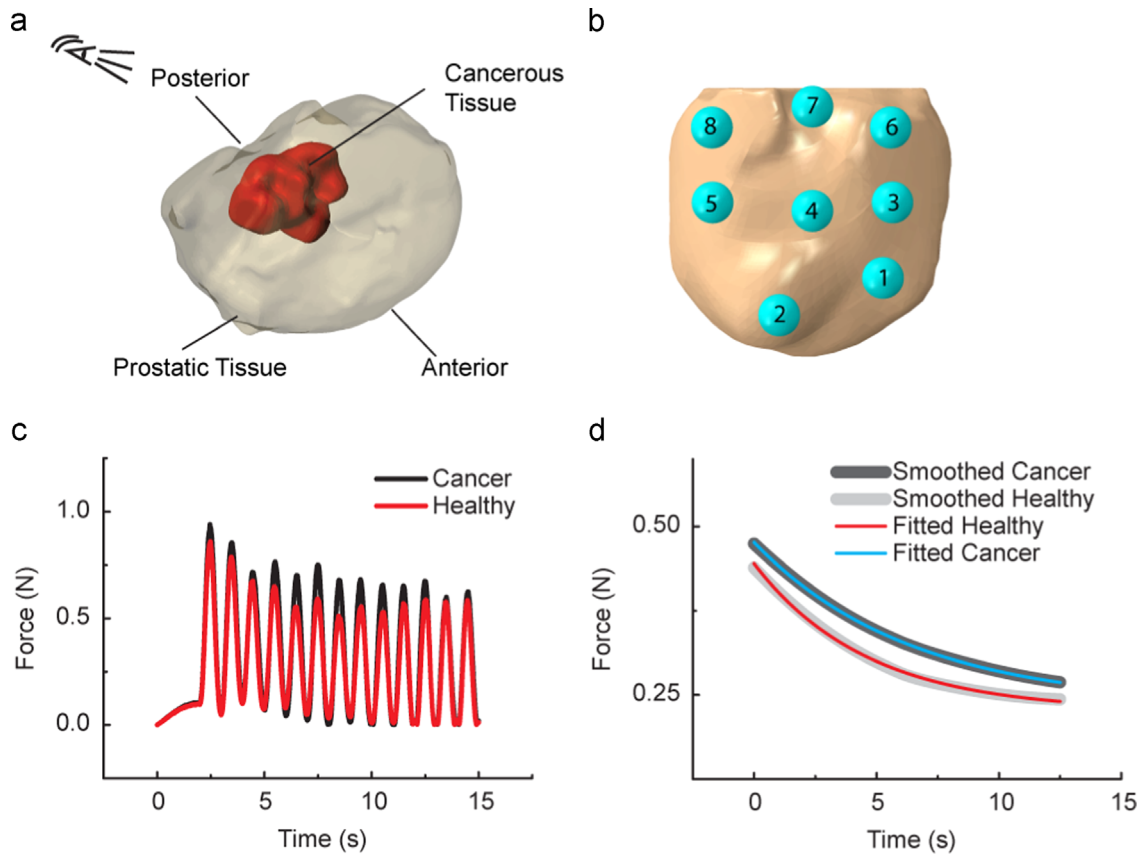
Fig. 8 – 3D prostate model obtained from the excised prostate specimen. (a) 3D prostate model from MRI scan; (b) 8 indentation sites at posterior surface; (c) Force feedback recorded during the indentation of the healthy prostate and the one with a cancerous nodule; and (d) smoothed data where viscoelastic parameters are fitted and obtained.

Table 3 – Viscoelastic parameters of the healthy and cancerous prostate at 8 indentation sites. The parameter τ serves as a better indicator of the tissue quality than a or b.

Position	Cancerous prostate			Healthy prostate			Relative change - (Cancerous-Healthy)/Healthy (%)		
	a	τ	b	a	τ	b	$\Delta a(\%)$	$\Delta \tau(\mathbf{TQI})(\%)$	$\Delta b(\%)$
1	0.3003	6.0309	0.3465	0.3049	6.2575	0.3395	−1.5087	−3.6213	2.0619
2	0.3082	6.4423	0.3120	0.3084	6.5138	0.3050	−0.0649	−1.0977	2.2951
3	0.2865	8.5801	0.2717	0.2903	8.7832	0.2621	−1.3090	−2.3124	3.6627
4	0.3670	5.9668	0.4163	0.3589	5.3558	0.4108	2.2569	11.4082	1.3389
5	0.2642	7.1316	0.4415	0.2451	6.4738	0.2721	7.7927	10.1610	62.2565
6	0.2440	7.4869	0.2530	0.2478	8.0876	0.2403	−1.5335	−7.4274	5.2851
7	0.3095	6.7779	0.3237	0.2817	5.9306	0.3109	9.8687	14.2869	4.1171
8	0.2456	8.6070	0.2661	0.2329	7.7745	0.2210	5.4530	10.7081	20.4072

4.   Concluding remarks

Based on the evidence from the literature that the viscoelasticity of soft tissue is affected by some pathological changes such as cancer, this paper has used published data for viscoelasticity of cancerous and healthy prostatic tissue to establish a novel framework for quantitative diagnostics for soft tissue using dynamic palpation.

The proposed method features diagnostic procedures that can be used to obtain elastic and viscous behaviors simultaneously, with the viscoelastic parameters being able to characterize the cancerous nodule, thus becoming a more reliable index for quantitative assessment of tissue quality. The method is illustrated on a 3D prostate model reconstructed from an MRI scan of an excised prostate. It is shown that the change of viscoelastic time constant between healthy and cancerous tissue, which defines the tissue quality index, could be a key indicator for quantitative diagnostics of tissue pathological conditions. Furthermore, the method presented here has certain advantages in a clinical context such as reduced duration of examination and less invasiveness. The
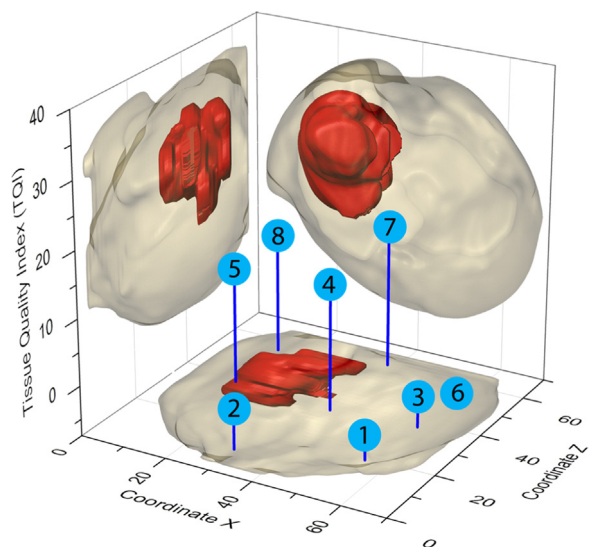
Fig. 9 – Tissue quality index (TQI) for the prostate with a cancerous nodule and the healthy one at 8 indentation sites.

proposed method is not limited to any particular material model or scale, and thus becomes useful for tissue where defining a unique time constant is not trivial. It is important to mention that the objective of this methodology is not to provide a very detailed description of the viscoelastic behavior. For that purpose, frequency testing as well as stress relaxation should be undertaken. Instead this study aims at providing a methodology to assess tissue quality in the framework of tissue diagnostics.

Assessment of other pathological conditions, such as benign prostate hyperplasia (BPH) and prostatitis in prostate tissue, will depend on their elastic properties and also the difference in viscoelastic time constant in comparison to healthy tissue. Selection of the indenter size and shape as well as indentation depth also requires further investigation to maximize the capability to assess tissue quality with enough resolution whilst still satisfying clinical constraints.

Acknowledgements

REFERENCES

Ahn, B., Kim, J., 2010. Measurement and characterization of soft tissue behavior with surface deformation and force response under large deformations. Med. Image Anal. 14, 138–148.

Ahn, B., Kim, Y., Oh, C.K., Kim, J., 2012. Robotic palpation and mechanical property characterization for abnormal tissue localization. Med. Biol. Eng. Comput. 50, 961–971.

Ahn, B., Lorenzo, E.I., Rha, K.H., Kim, H.J., Kim, J., 2011. Robotic palpation-based mechanical property mapping for diagnosis of prostate cancer. J. Endourol./Endourological Soc. 25, 851–857.

Ahn, B.M., Kim, J., Ian, L., Rha, K.H., Kim, H.J., 2010. Mechanical property characterization of prostate cancer using a minimally motorized indenter in an ex vivo indentation experiment. Urology 76, 1007–1011.

Ali, A., Hosseini, M., Shara, B.B., 2010. A review of constitutive models for rubber-like materials. Am. J. Eng. Appl. Sci. 3, 232–239.

Anssari-Benam, A., Bader, D.L., Screen, H.R., 2011. A combined experimental and modelling approach to aortic valve viscoelasticity in tensile deformation. J. Mater. Sci.—Mater. Med. 22, 253–262.

Balleyguier, C., Canale, S., Ben Hassen, W., Vielh, P., Bayou, E.H., Mathieu, M.C., Uzan, C., Bourgier, C., Dromain, C., 2013. Breast elasticity: principles, technique, results: an update and overview of commercially available software. Eur. J. Radiol. 82, 427–434.

Bates, J.H., 2007. A recruitment model of quasi-linear power-law stress adaptation in lung tissue. Ann. Biomed. Eng. 35, 1165–1174.

Bayliss, L.E., Robertson, G.W., 1939. The visco-elastic properties of the lungs. Q. J. Exp. Physiol. 29, 27–47.

Beda, T., 2007. Modeling hyperelastic behavior of rubber: a novel invariant-based and a review of constitutive models. J. Polym. Sci., Part B: Polym. Phys. 45, 1713–1732.

Bergström, J.S., Boyce, M.C., 2001. Constitutive modeling of the time-dependent and cyclic loading of elastomers and application to soft biological tissues. Mech. Mater. 33, 523–530.

Bergström, J.S., Boyce, M.C., 1997. Constitutive modeling of the large strain time-dependent behavior of elastomers. J. Mech. Phys. Solids 46, 931–954.

Bischoff, J.E., 2006. Reduced parameter formulation for incorporating fiber level viscoelasticity into tissue level biomechanical models. Ann. Biomed. Eng. 34, 1164–1172.

Boyce, M.C., Arruda, E.M., 2000. Constitutive models of rubber elasticity: a review. Rubber Chem. Technol. 73, 504–523.

Brinson, H.F., Brinson, L.C., 2008. Polymer Engineering Science and Viscoelasticity: An Introduction. Springer Science+Business Media, Spring Street, New York, NY 10013, USA (LLC, 233).

Carson, W.C., Gerling, G.J., Krupski, T.L., Kowalik, C.G., Harper, J.C., Moskaluk, C.A., 2011. Material characterization of ex vivo prostate tissue via spherical indentation in the clinic. Med. Eng. Phys. 33, 302–309.

Carter, F.J., Frank, T.G., Davies, P.J., McLean, D., Cuschieri, A., 2001. Measurements and modelling of the compliance of human and porcine organs. Med. Image Anal. 5, 231–236.

Chen, L.H., Ng, S.P., Yu, W., Zhou, J., Wan, K.W., 2013. A study of breast motion using non-linear dynamic FE analysis. Ergonomics 56, 868–878.

Cleveland, W.S., 1979. Robust locally weighted regression and smoothing scatterplots. J. Am. Stat. Assoc. 74, 829–836.

Ebihara, T., Venkatesan, N., Tanaka, R., Ludwig, M., 2000. Changes in extracellular matrix and tissue viscoelasticity in bleomycin–induced lung fibrosis. Am. J. Respir. Crit. Care Med. 162, 1569–1576.

Garteiser, P., Doblas, S., Daire, J.L., Wagner, M., Leitao, H., Vilgrain, V., Sinkus, R., Van Beers, B.E., 2012. MR elastography of liver tumours: value of viscoelastic properties for tumour characterisation. Eur. Radiol. 22, 2169–2177.

Gasser, T.C., Holzapfel, G.A., 2002. A rate-independent elastoplastic constitutive model for biological fiber-reinforced

composites at finite strains: continuum basis, algorithmic formulation and finite element implementation. Comput. Mech. 29, 340–360.

Guo, J., Hirsch, S., Fehlner, A., Papazoglou, S., Scheel, M., Braun, J., Sack, I., 2013. Toward an elastographic atlas of brain anatomy. PLoS One.

Holzapfel, G.A., 2000. Biomechanics of soft tissue. In: Lemaitre, J. (Ed.), Handbook of Material Behavior, Nonlinear Models and Properties. LMT-Cachan, France.

Holzapfel, G.A., Gasser, T.C., 2000. A viscoelastic model for fiber-reinforced composites at finite strains: continuum basis, computational aspects and applications. Comput. Meth. Appl. Mech. Eng. 190, 4379–4403.

Holzapfel, G.A., Gasser, T.C., Ogden, R.W., 2000. A new constitutive framework for arterial wall mechanics and a comparative study of material models. J. Elast. 61, 1–48.

Hoyt, K., Castaneda, B., Zhang, M., Nigwekar, P., Anthony di Sant'Agnese, P., Joseph, J.V., Strang, J., Rubens, D.J., Parker, K.J., 2008. Tissue elasticity properties as biomarkers for prostate cancer. Cancer Biomarkers 4, 213–225.

Huang, C.Y., Mow, V.C., Ateshian, G.A., 2001. The role of flow-independent viscoelasticity in the biphasic tensile and compressive responses of articular cartilage. J. Biomech. Eng. 123, 410.

Kerdok, A.E., Ottensmeyer, M.P., Howe, R.D., 2006. Effects of perfusion on the viscoelastic characteristics of liver. J. Biomech. 39, 2221–2231.

Klatt, D., Hamhaber, U., Asbach, P., Braun, J., Sack, I., 2007. Noninvasive assessment of the rheological behavior of human organs using multifrequency MR elastography: a study of brain and liver viscoelasticity. Phys. Med. Biol. 52, 7281–7294.

Krouskop, T.A., Wheeler, T.M., Kallel, F., Garra, B.S., Hall, T., 1998. Elastic moduli of breast and prostate tissues under compression. Ultrason. Imaging 20, 260–274.

Madsen, E.L., Hobson, M.A., Shi, H., Varghese, T., Frank, G.R., 2005. Tissue-mimicking agar/gelatin materials for use in heterogeneous elastography phantoms. Phys. Med. Biol. 50, 5597–5618.

Martinez-Agirre, M., Elejabarrieta, M.J., 2011. Dynamic characterization of high damping viscoelastic materials from vibration test data. J. Sound Vib. 330, 3930–3943.

Masuzaki, R., Tateishi, R., Yoshida, H., Sato, T., Ohki, T., Goto, T., Yoshida, H., Sato, S., Sugioka, Y., Ikeda, H., Shiina, S., Kawabe, T., Omata, M., 2007. Assessing liver tumor stiffness by transient elastography. Hepatol. Int. 1, 394–397.

Miller, K., Chinzei, K., Orssengo, G., Bednarz, P., 2000. Mechanical properties of brain tissue in-vivo: experiment and computer simulation. J. Biomech. 33, 1369–1376.

Murayama, Y., Nihon Univ., F., Omata, S.Y., T., Qiyu Peng; Shishido, K.; Peehl, D.M.; Constantinou, C.E., 2007. High resolution regional elasticity mapping of the human prostate. In: 29th Annual International Conference of the IEEE, Cite Internationale, Lyon, France, pp. 5802–5805.

Nayar, V.T., Weiland, J.D., Nelson, C.S., Hodge, A.M., 2012. Elastic and viscoelastic characterization of agar. J. Mech. Behav. Biomed. Mater. 7, 60–68.

Oflaz, H., Baran, O., 2014. A new medical device to measure a stiffness of soft materials. Acta Bioeng Biomech. 16, 125–131.

Pailler-Mattei, C., Bec, S., Zahouani, H., 2008. In vivo measurements of the elastic mechanical properties of human skin by indentation tests. Med. Eng. Phys. 30, 599–606.

Palacio, J., Jorge-Penas, A., Munoz-Barrutia, A., Ortiz-de-Solorzano, C., de Juan-Pardo, E., Garcia-Aznar, J.M., 2013. Numerical estimation of 3D mechanical forces exerted by cells on non-linear materials. J. Biomech. 46, 50–55.

Park, S.W., Schapery, R.A., 1999. Methods of interconversion between linear viscoelastic material functions. Part I—A numerical method based on Prony series. Int. J. Solids Struct. 36, 1653–1675.

Peña, E., Alastrue, V., Laborda, A., Martinez, M.A., Doblare, M., 2010. A constitutive formulation of vascular tissue mechanics including viscoelasticity and softening behaviour. J. Biomech. 43, 984–989.

Phipps, S., Yang, T.H., Habib, F.K., Reuben, R.L., McNeill, S.A., 2005. Measurement of the mechanical characteristics of benign prostatic tissue: a novel method for assessing benign prostatic disease. Urology 65, 1024–1028.

Rashid, B., Destrade, M., Gilchrist, M.D., 2014. Mechanical characterization of brain tissue in tension at dynamic strain rates. J. Mech. Behav. Biomed. Mater. 33, 43–54.

Renaud, F., Dion, J.L., Chevallier, G., Tawfiq, I., Lemaire, R., 2011. A new identification method of viscoelastic behavior: application to the generalized Maxwell model. Mech. Syst. Sig. Process. 25, 991–1010.

Sack, I., Beierbach, B., Wuerfel, J., Klatt, D., Hamhaber, U., Papazoglou, S., Martus, P., Braun, J., 2009. The impact of aging and gender on brain viscoelasticity. NeuroImage 46, 652–657.

Sack, I., Jöhrens, K., Würfel, J., Braun, J., 2013. Structure-sensitive elastography: on the viscoelastic powerlaw behavior of in vivo human tissue in health and disease. Soft Matter 9, 5672.

Salameh, N., Peeters, F., Sinkus, R., Abarca-Quinones, J., Annet, L., ter Beek, L.C., Leclercq, I., Van Beers, B.E., 2007. Hepatic viscoelastic parameters measured with MR elastography: correlations with quantitative analysis of liver fibrosis in the rat. J. Magn. Reson. Imaging 26, 956–962.

Sangpradit, K., Liu, H.b., Dasgupta, P., Althoefer, K., Seneviratne, L.D., 2011. Finite-element modeling of soft tissue rolling indentation. IEEE Trans. Biomed. Eng. 58, 3319–3327.

Sartor, A.O., Hricak, H., Wheeler, T.M., Coleman, J., Penson, D.F., Carroll, P.R., Rubin, M.A., Scardino, P.T., 2008. Evaluating localized prostate cancer and identifying candidates for focal therapy. Urology 72, S12–S24.

Silver-Thorn, M.B., 1999. In vivo indentation of lower extremity limb soft tissues. IEEE Trans. Neural Syst. Rehabil. Eng. 7, 268–277.

Sinkus, R., Tanter, M., Xydeas, T., Catheline, S., Bercoff, J., Fink, M., 2005. Viscoelastic shear properties of in vivo breast lesions measured by MR elastography. Magn. Reson. Imaging 23, 159–165.

Soltz, M.A., Ateshian, G.A., 1998. Experimental verification and theoretical prediction of cartilage interstitial fluid pressurization at an impermeable contact interface in confined compression. J. Biomech. 31, 927–934.

Streitberger, K.-J., Sack, I., Krefting, D., Pfueller, C., Braun, J., Paul, F., Wuerfel, J., 2012. Brain viscoelasticity alteration in chronic-progressive multiple sclerosis. PLoS One.

Su, L.M., 2010. Early Diagnosis and Treatment of Cancer. Saunders Elsevier.

Takaza, M., Moerman, K.M., Gindre, J., Lyons, G., Simms, C.K., 2013. The anisotropic mechanical behaviour of passive skeletal muscle tissue subjected to large tensile strain. J. Mech. Behav. Biomed. Mater. 17, 209–220.

Taylor, S.L., Lerner, A.L., Rubens, D.J., Parker, K.J., 2002. A Kelvin-Voigt Fractional Derivative Model For Viscoelastic Characterization of Liver Tissue. ASME International Mechanical Engineering Congress & Exposition, New Orleans, Louisiana.

Torlakovic, G., Grover, V.K., Torlakovic, E., 2005. Easy method of assessing volume of prostate adenocarcinoma from estimated tumor area: using prostate tissue density to bridge gap between percentage involvement and tumor volume. Croat. Med. J. 46, 423–428.

Tran, A.B., Yvonnet, J., He, Q.C., Toulemonde, C., Sanahuja, J., 2011. A simple computational homogenization method for structures made of linear heterogeneous viscoelastic materials. Comput. Meth. Appl. Mech. Eng. 200, 2956–2970.

Van Loocke, M., Simms, C.K., Lyons, C.G., 2009. Viscoelastic properties of passive skeletal muscle in compression-cyclic behaviour. J. Biomech. 42, 1038–1048.

Xu, F., Wen, T., Seffen, K.A., Lu, T.J., 2007. Characterization of thermomechanical behaviour of skin tissue II. In: Viscoelastic Behaviour, World Congress on Engineering 2007 V, London.

Yarpuzlu, B., Ayyildiz, M., Tok, O.E., Aktas, R.G., Basdogan, C., 2014. Correlation between the mechanical and histological properties of liver tissue. J. Mech. Behav. Biomed. Mater. 29, 403–416.

Yu, P., Haddad, Y.M., 1994. On the dynamic system identification of the response behaviour of linear viscoelastic materials. Int. J. Press. Vessels Pip. 67, 45–54.